Hydrogen Storage Issues for Automotive Fuel Cells

JoAnn Milliken, U.S. Department of Energy
John Petrovic, Los Alamos National Laboratory
Walter Podolski, Argonne National Laboratory

International Workshop on Hydrogen in Materials and Vacuum Systems
11-13 November 2002
Jefferson Lab
Newport News, Virginia

On-Board Hydrogen Storage Challenge

Storing enough hydrogen on vehicles to achieve greater than 300 miles driving range is difficult.

- **On a weight basis H_2 has nearly three times the energy content of gasoline.**
  - **120 MJ/kg vs. 44 MJ/kg (LHV)**
- **On a volume basis the situation is reversed.**
  - **3 MJ/L (5000 psi), 8 MJ/L (LH_2) vs. 32 MJ/L**
- **Physical storage of hydrogen is bulky.**
- **Capacity of reversible chemical storage at useful T, P is low.**
- **Other challenging issues include energy efficiency, cost, and safety.**

2010 DOE Technical Targets for On-Board Hydrogen Storage

TO BE REVISED

	Units	Target
Storage Weight Percent	%	6
Energy Efficiency	%	97
Energy Density	W-h/L	1100
Specific Energy	W-h/kg	2000
Cost	$/kW-h	5
Operating Temperature	°	-40–50°C
Start-Up Time To Full Flow	sec	15
Hydrogen Loss	scc/hr/L	1.0
Cycle Life	Cycles	500
Refueling Time	min	<5
Recoverable Usable Amount	%	90

DOE Hydrogen Storage Approaches

- Compressed and liquid hydrogen tanks
- Chemical hydrides
- Carbon structures
- Complex metal hydrides

Compressed/Liquid Hydrogen Storage

Compressed H_2 Storage

Type IV all-composite tanks are available at 5000 psi (350 bar); prototype 10,000 psi tanks completed EIHP-based certification tests.

Packaging volume is still a concern.

Liquid H_2 Storage

- Liquifying H_2 requires substantial energy (40% of HHV)
- Boil-off is an issue for non-pressurized insulated tanks
- Pressurized cryogenic tanks are being developed by LLNL.

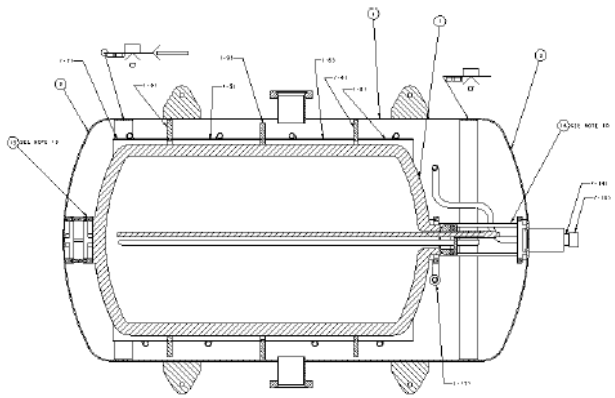

Hydrogen Storage Workshop
14-15 August 2002
Argonne National Laboratory

The focus of the workshop was on storage materials, with careful consideration of system level requirements.

- **Identify and prioritize the most promising approaches to development of viable hydrogen storage materials/technologies**
- **Identify the technical challenges related to those approaches**
- **Draft a research and development plan to overcome those challenges**

Overarching R&D Questions for All Advanced Materials

- Maximum storage capacity – theoretical model
- Energy balance / life cycle analysis
- Hydrogen absorption / desorption kinetics
- Preliminary cost analysis –
  potential for low cost, high volume
- Safety

Workshop Format

- Argonne National Laboratory
  - August 14-15, 2002
  - Attendees
    - 49 DOE/Laboratory
    - 32 Industry
    - 16 University
  - Plenary session
    - Overview of DOE Program
    - Automaker's perspective
    - Four technology overview presentations
  - Four breakout groups
    - Advanced/complex hydrides
    - Chemical storage
    - Carbon storage
    - Advanced concepts

General Motors
Gravimetric Energy Density vs. Volumetric Energy Density of Fuel Cell Hydrogen Storage Systems

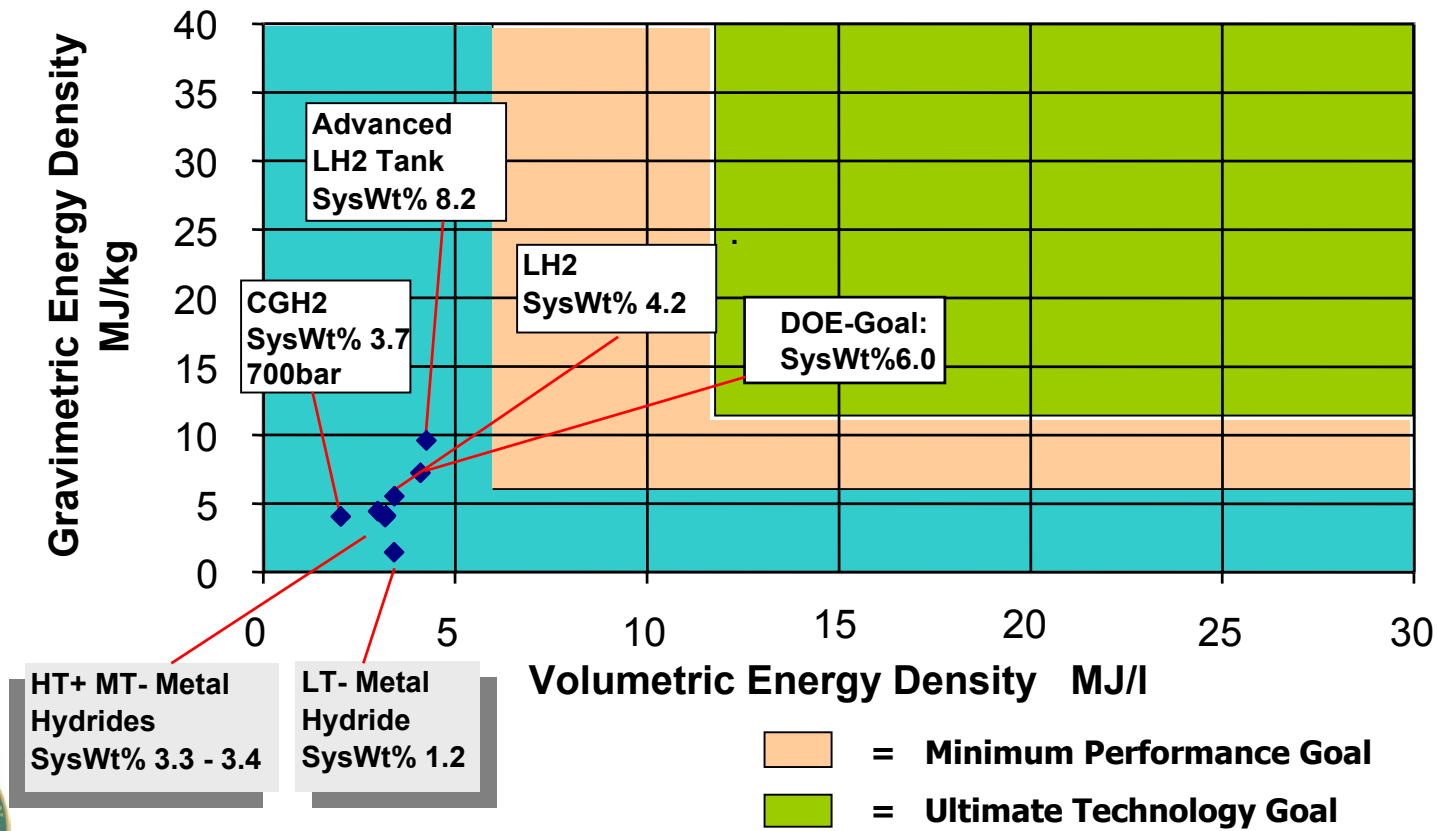

DOE target is too low.

Reversible Metal Hydride System

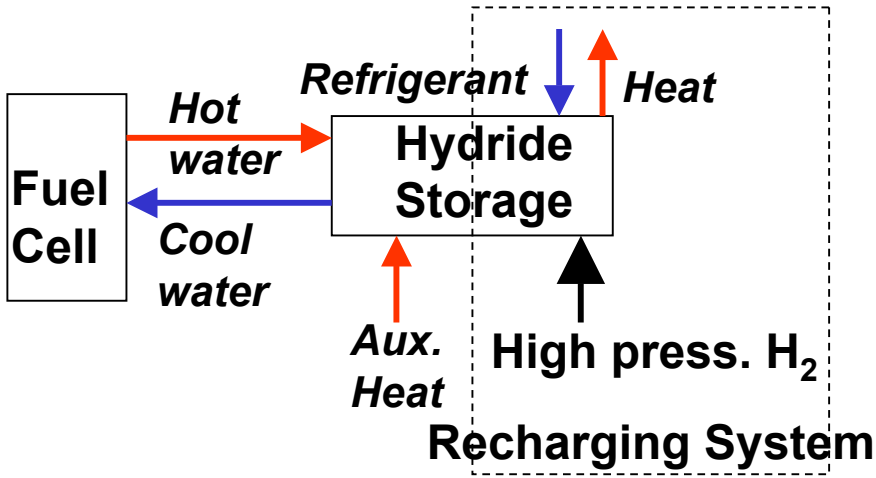

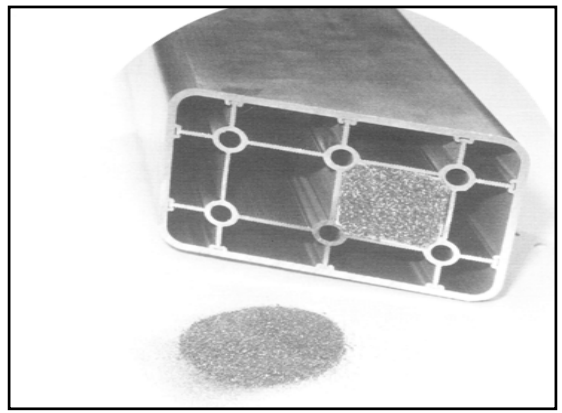

Sodium alanate doped with Ti is reversible but not quite suitable for vehicle applications.

$$3NaAlH_4 \rightleftarrows Na_3AlH_6 + 2Al + 3H_2 \rightleftarrows 3NaH + Al + 3/2H_2$$

3.7 wt% *1.8 wt%*

PEM fuel cell exhaust is near 80°C. Capacity and kinetics are too low.

Metal Hydrides Conclusions/Recommendations

Conclusions

- $NaAlH_4$ capacity limited to about 5.6 wt%
  - Interim goal (5-year) of 6 wt%
- Need 8 wt% hydrogen material capacity if BOP adds 20%

Recommendations

- Continue fundamental studies on $NaAlH_4$ as model system
- Identify other hydride materials that have storage capacity greater than 6 wt%
- Develop new materials to achieve 8 wt%
- Engineering analyses
  - Preliminary system cost analysis
  - Large scale material production
  - Independent safety consultant/laboratory to understand safety and certification issues

Chemical Hydrides

Three Approaches

$$NaBH_4 + 2H_2O \rightarrow NaBO_2 + 4H_2$$

Millenium Cell
DaimlerChrysler

20 - 35% sol. Stabilized with 1-3% NaOH

Proprietary catalyst

Borax in NaOH

$$2LiH + 2H_2O \rightarrow 2LiOH + 2H_2$$

ThermoPower

Light mineral oil slurry, proprietary stabilizers

Paste byproduct

Capacity is around 10 wt%, reduced by other materials.
Dehydrogenation kinetics are fast.
Reactions are irreversible on board vehicle.

$$2Na + 2H_2O \rightarrow 2NaOH + H_2$$

Powerball

Polyethylene-coated pellets, mechanically cut to expose Na

Chemical Hydride R&D Recommendations

- Screen chemical complexes
  - Hydrogen storage density potential
  - Thermodynamic energy requirements including regeneration
- Improved/new process chemistry
  - Catalysts
  - Operating conditions (temperature, pressure)
- Well-to-wheels-to-well analysis of top complexes
  - Primary energy use
  - Cost of delivered fuel
  - Emissions
  - Resource depletion

Single-Wall Carbon Nanotubes

- Capacity around 4 wt%
- Doped SWNTs to 7 wt% by NREL
- Ambient temperature, moderate pressure
- SWNTs are made by arc discharge, laser vaporization, CVD, and lithographically
- SWNTs must be purified, cut, and the ends opened

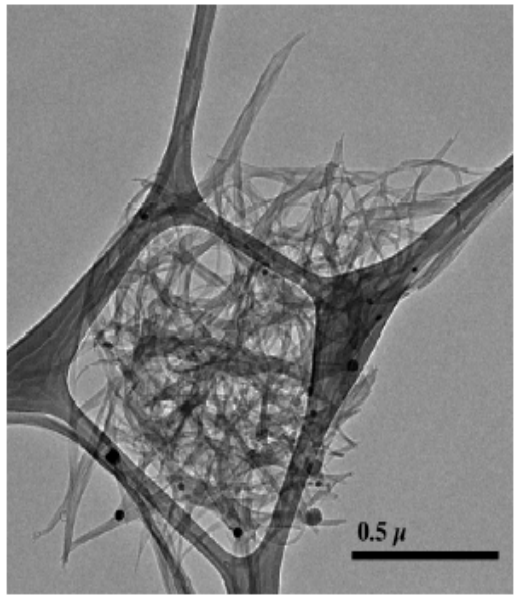

Reproducibility is a critical issue.

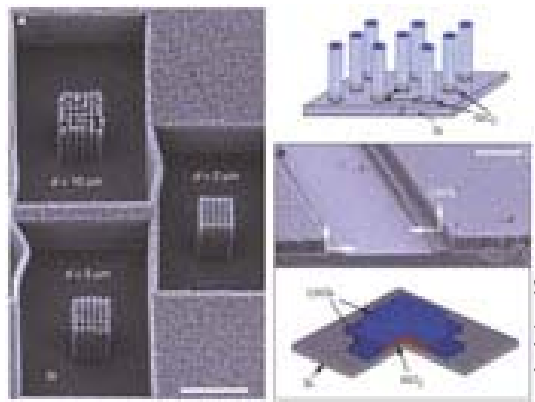

Wei, B. Q., et al, Nature, Vol. 416, April 2002

Carbon R&D Recommendations

- Conduct definitive experiments to show where and how hydrogen is stored in SWNT and for various forms of carbon
  - develop 2-3 pure SWNT standards for synthesis, purification, activation, and hydrogen adsorption/desorption
  - conduct round-robin testing
    - role of SWRI, other labs, universities, industry

- Better understand the science to engineer carbon for hydrogen storage
  - Baseline theory to elucidate parameters affecting the number and type of binding sites and heat of reaction for a broad range of modified carbon materials
  - Provide "directional" guidance for experiments (and vice-versa)

Advanced Concepts Identified

1. Crystalline Nanoporous Materials
2. Polymer Microspheres
   Self-Assembled Nanocomposites
3. Advanced Hydrides
4. Metals – Organic
5. BN Nanotubes
   Hydrogenated Amorphous Carbon
6. Mesoporous materials
7. Bulk Amorphous Materials (BAMs)
8. Iron Hydrolysis
9. Nanosize powders
10. Metallic Hydrogen
    Hydride Alcoholysis

Advanced Hydride Materials

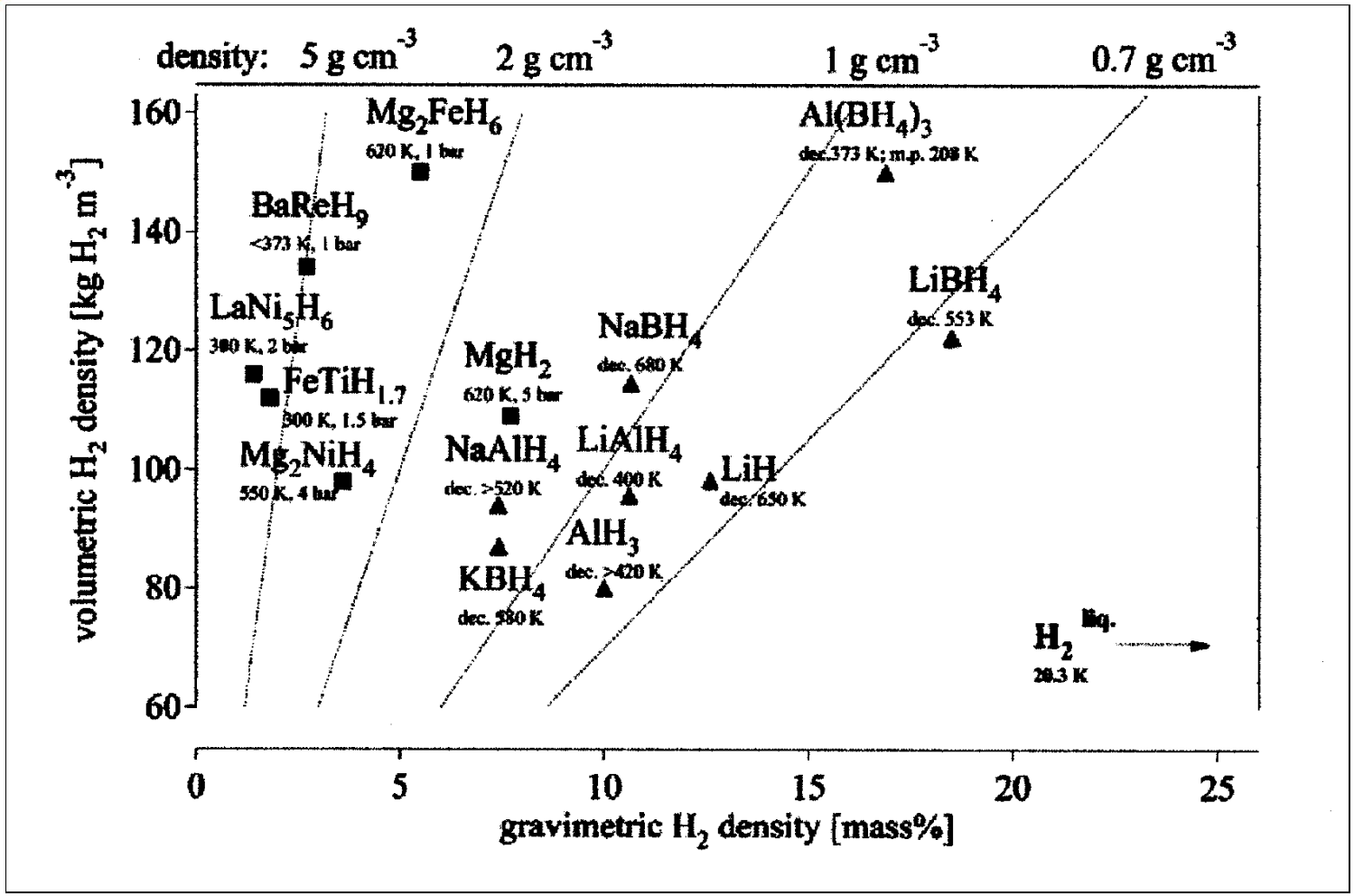

A. Zuttel, et.al., "Hydrogen Desorption From Lithiumtetrahydroboride ($LiBH_4$), Proceedings, 14th World Hydrogen Energy Conference, June 2002, Montreal, Canada.

Hydrogen Generation from $LiBH_4$

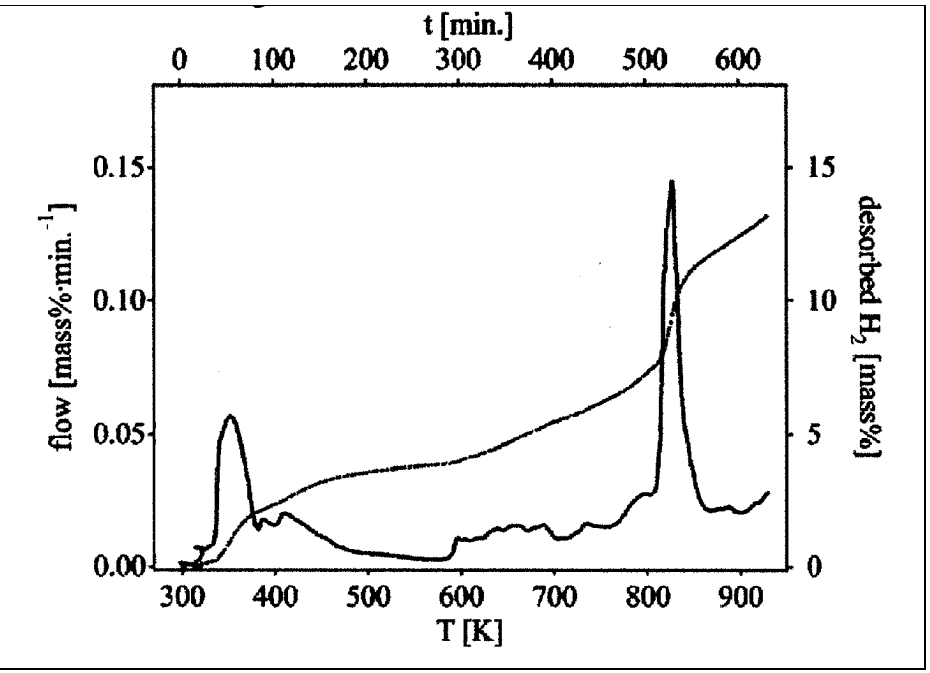

- $LiBH_4$ (lithium tetrahydroboride)
  - Salt-like, hydroscopic, crystalline material
  - Density 0.68 g/cm^3
  - Melting point 275 ^oC
- $LiBH_4 = LiH + B + 1.5H_2(g)$
  - ΔG becomes negative at 450 ^oC
  - Endothermic reaction
  - 13.8 wt.% H_2 released
- A low temperature H_2 release has been observed
  - 2.3 wt.% H_2 released at 118 ^oC
  - May be related to an orthorhombic-to-tetragonal crystallographic change
    - Is this a reversible process?

A. Zuttel, et.al., "Hydrogen Desorption From Lithiumtetrahydroboride ($LiBH_4$), Proceedings, 14th World Hydrogen Energy Conference, June 2002, Montreal, Canada.

Hydrolysis of $LiBH_4$-Organics

Organics combined with $LiBH_4$ to reduce the severity and heat of the hydrolysis reaction

$$\{M(L)BH_4\}_x + 4xH_2O \rightarrow 4xH_2 + xMOH + xB(OH)_3 + xL$$

M = lithium
L = organic ligand

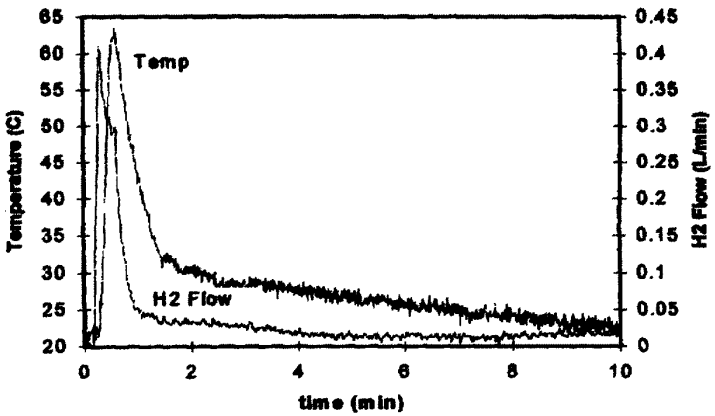

Fig. 3. Data acquired in the hydrolysis of compound 2.

Molecular weight of organics in the range of 300 g/mol

Table 3. Hydrogen yields and maximum temperatures

Compound	$NaBH_4$	1	2	3	4	5	6
Hydrogen Yield[a] (% of theoretical)	89, 96	88, 100	98	56, 68	84	76, 87	104, 101
Maximum Temp (°C)	87, 98	52, 67	63	84, 54	60	45, 45	55, 36

(1) $[HC(3,5\text{-}Me_2pz)_3]LiBH_4$; (2) $\{[H_2C(3,5\text{-}Me_2pz)_2]Li(BH_4)\}_2$; (3) $[(TMEDA)Li(BH_4)]_2$; (4) $[HC(pz)_3]LiBH_4$; (5) $\{[H_2C(pz)_2]Li(BH_4)\}_2$; (6) $Mg(BH_4)_2 \cdot 3THF$.
[a] accuracy is estimated to be ±5%.

Table 2. Heats of hydrolysis reaction of the novel hydrides

Compound	$NaBH_4$	$LiBH_4$	1	2	4	5	6
kJ mol hydride	−267	−301	−255	−284	−216	−435	−414
kJ mol H_2 produced	−67	−75	−64	−36	−54	−54	−52
kJ kg reactants	−2431	−3211	−650	−477	−699	−898	−1000
kJ l reactants	−2496	−2879	−692	−509	−753	−995	−1200

(1) $[HC(3,5\text{-}Me_2pz)_3]LiBH_4$; (2) $\{[H_2C(3,5\text{-}Me_2pz)_2]Li(BH_4)\}_2$; (3) $[(TMEDA)Li(BH_4)]_2$; (4) $[HC(pz)_3]LiBH_4$; (5) $\{[H_2C(pz)_2]Li(BH_4)\}_2$; (6) $Mg(BH_4)_2 \cdot 3THF$.

2.5 wt.% H_2 produced from Compound 1

R. Aiello, M.A. Matthews, D.L. Reger, and J.E. Collins, "Production of Hydrogen Gas From Novel Chemical Hydrides", Int. J. Hydrogen Energy, 23, 1103-1108 (1998).

Chemical Reactions of Hydrides With Alcohols (Alcoholysis)

Hydride	wt. % of H_2 (in respect to the hydride weight)	Litres of H_2 obtained per 1 kg of hydride	Total H_2 capacity (including the weight of the hydride **and** the alcohol - methanol)
LiH	25.4	2845	5.0
$LiAlH_4$	13.2	1478	7.2
Li_3AlH_6	16.8	1882	6.1
$LiBH_4$	23.1	2592	9.4
NaH	8.3	933	3.6
$NaAlH_4$	9.3	1045	5.9
Na_3AlH_6	8.9	996	4.6
$NaBH_4$	13.3	1490	7.3
$Li_3Be_2H_7$	22.0	2460	7.1
Li_2BeH_4	22.5	2516	6.7
MgH_2	15.3	1716	4.5
CaH_2	9.6	1074	3.8
$FeTiH_2$	5.7	641	2.6
ZrH_2	4.3	484	2.6
TiH_2	8.1	905	3.5
$MgAl_2H_8$	11.7	1307	6.7
$LiAl_2H_7$	11.9	1329	8.1
$ZrAl_2H_8$	6.6	737	4.6

$$MH_x + x\,ROH \Rightarrow M(OR)_x + x\,H_2\uparrow$$

$$LiH + CH_3OH \rightarrow LiOCH_3 + H_2$$

$$NaH + CH_3OH \rightarrow NaOCH_3 + H_2$$

$$LiH + C_2H_5OH \rightarrow LiOC_2H_5 + H_2$$

$$MgH_2 + 2\,C_2H_5OH \rightarrow Mg(OC_2H_5)_2 + 2\,H_2$$

Controlled and convenient production of H_2 at room temperature and below

John Strom-Olsen, "Method of Hydrogen Generation for Fuel Cell Applications and a Hydrogen-Generating System", Patent Filing WO0185606, May 2001, McGill University.

Hydrogen Adsorption by Boron Nitride Nanotubes

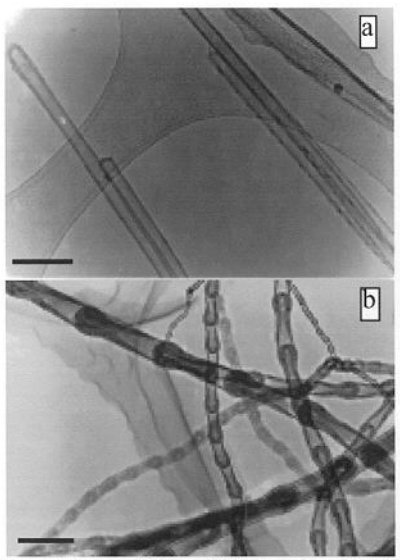

Figure 1 The morphologies of BN nanotubes: (a) multiwall nanotubes and (b) bamboo-like nanotubes. Scale bar: 100 nm.

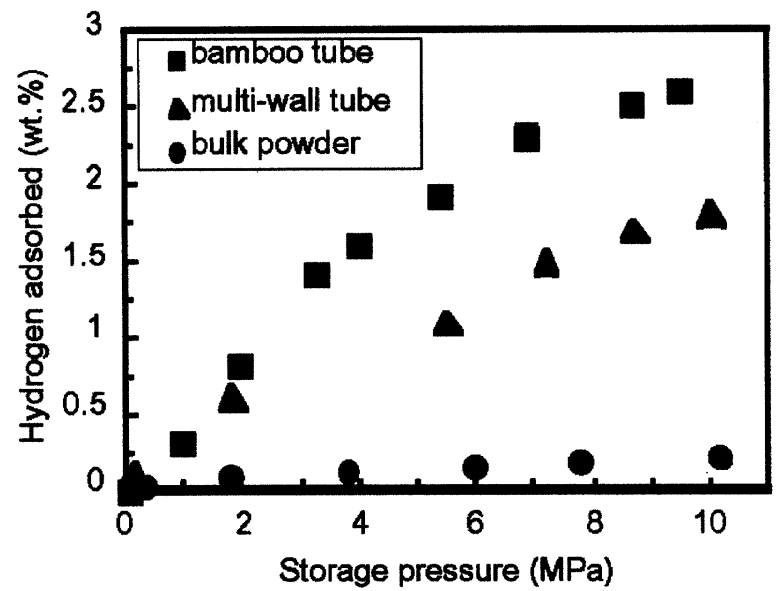

Figure 2 The hydrogen adsorption as a function of pressure in multiwall BN nanotubes and bamboo nanotubes at ~10 MPa is 1.8 and 2.6 wt %, respectively, in sharp contrast to the 0.2 wt % in bulk BN powder. The values reported here have an error of <0.3 wt %.

R. Ma, Y. Bando, H.Zhu, T. Sato, C. Xu, and D. Wu, "Hydrogen Uptake in Boron Nitride Nanotubes at Room Temperature", J. Am. Chem. Soc., 124, 7672-7673 (2002).

Zeolite Structures

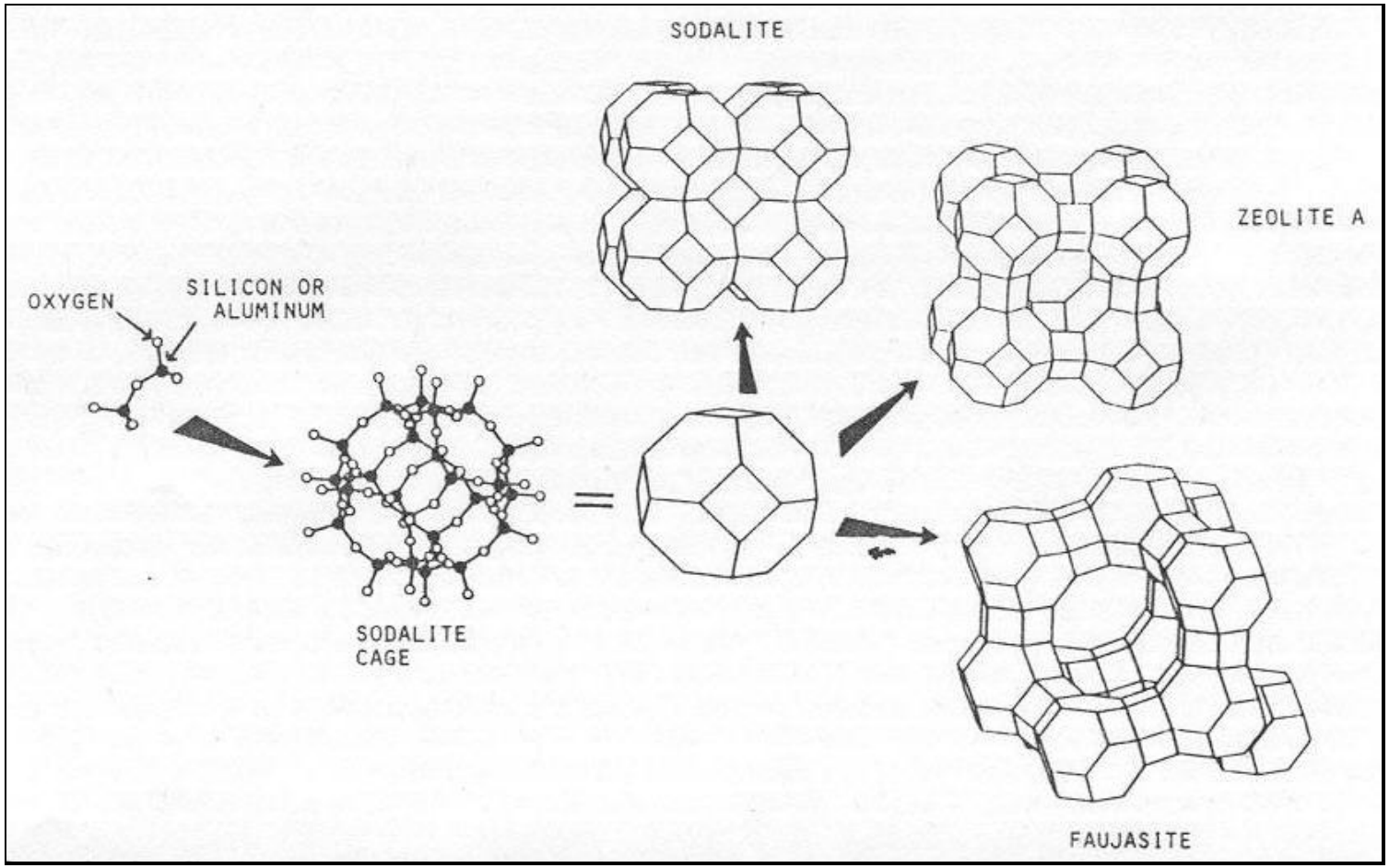

M.E. Davis, "Zeolites and Molecular Sieves: Not Just Ordinary Catalysts", Ind. Eng. Chem. Res., 30, 1675-1683 (1991).

Comparison of Carbon and Zeolite Hydrogen Physisorption

- Physisorption at 77 ^{o}K and 1 bar pressure
- Activated carbon Norit 990293
  - BET surface area 2030 m^2/gm
  - 2.1 wt.% hydrogen adsorbed
    - Highest level of all carbon materials that were examined
- Zeolite ZSM-5
  - BET surface area 430 m^2/gm
  - 0.7 wt.% hydrogen adsorbed
    - Highest level of all silica-based materials that were examined

M.G. Nijkamp, J.E. Raaymakers, A.J. van Dillen, and K.P. de Jong, "Hydrogen Storage Using Physisorption – Materials Demands", Appl. Phys. A, 72, 619-623 (2001).

Zeolite A

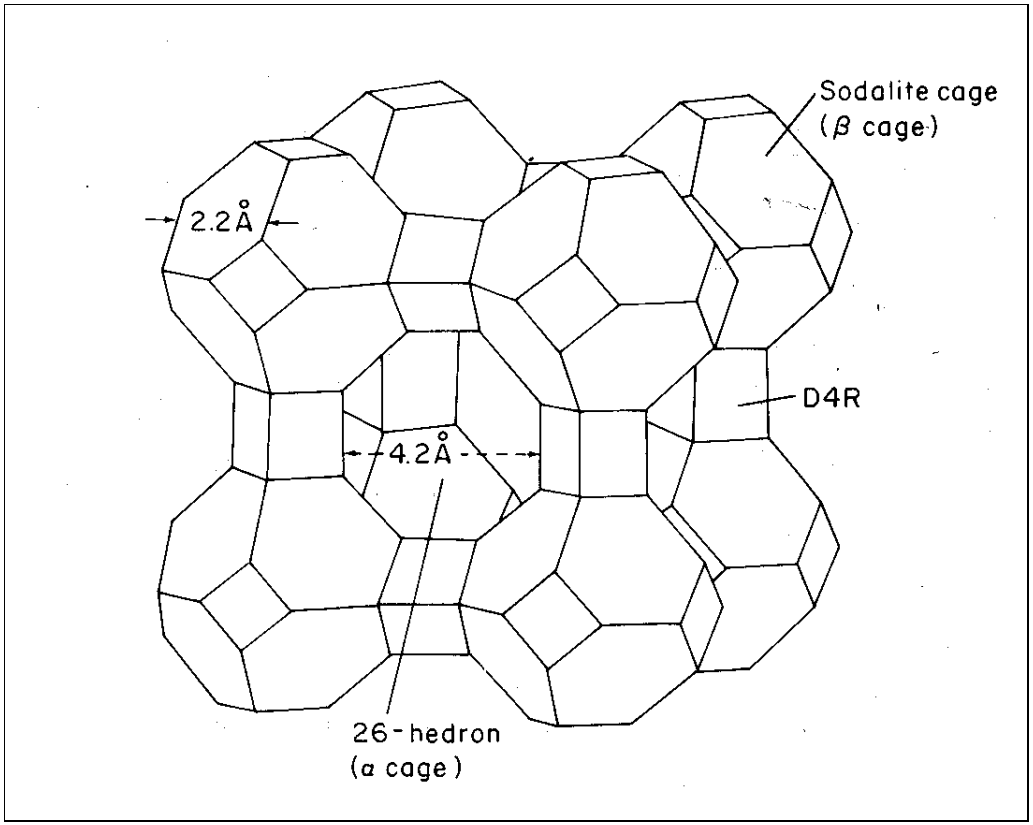

- $\{Na_{12}[Al_{12}Si_{12}O_{48}]\}_8$
- 8-ring channel
- Three-dimensional channels along <100> directions
- Channel diameter 0.42 nm

M.E. Davis, "Zeolites and Molecular Sieves: Not Just Ordinary Catalysts", Ind. Eng. Chem. Res., 30, 1675-1683 (1991).

Hydrogen Storage In Zeolite A

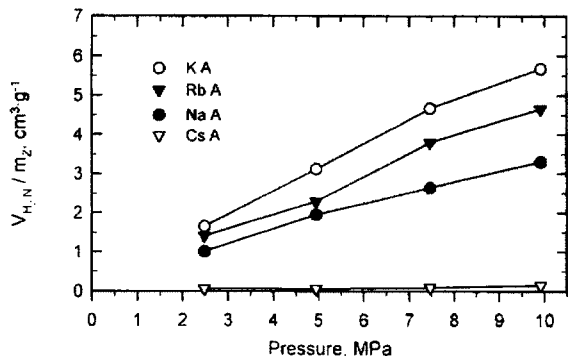

Fig. 1. Influence of pressure on the amount of encapsulated hydrogen in zeolites KA, NaA, RbA and CsA. Loading conditions: temperature—573 K; time—15 min.; $V_{H_2,N}$ denotes the volume of stored hydrogen at 273.15 K and 101.3 kPa; and m_Z the mass of the dry zeolite.

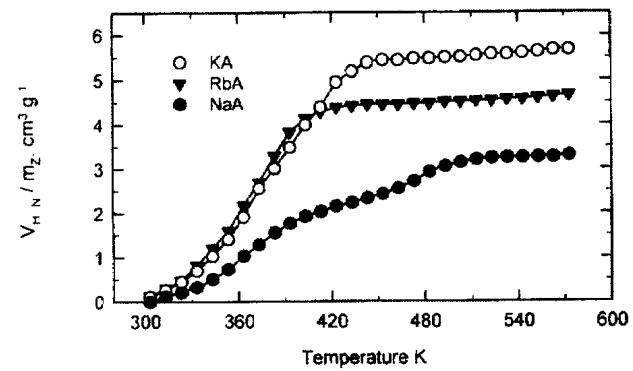

Fig. 5. Release of encapsulated hydrogen from zeolites NaA, KA and RbA upon heating at a rate of 15 K/min to 573 K.

- 0.05 wt.% H_2 was reversibly stored in Zeolite A at 300 ^oC
- H_2 molecules believed to be stored in the sodalite cages
  - Only 20-25% of sodalite cages contained an H_2 molecule
    - Reasons for this partial cage filling were unclear
- Can zeolites be chemically designed to store significantly more hydrogen?
  - H_2 molecules stored in <u>both</u> sodalite and α cages

J. Weitkamp, M. Fritz, and S. Ernst, "Zeolites as Media for Hydrogen Storage", International Journal of Hydrogen Energy, <u>20</u>, 967-970 (1995).

Modeling of Hydrogen Storage in Zeolite A

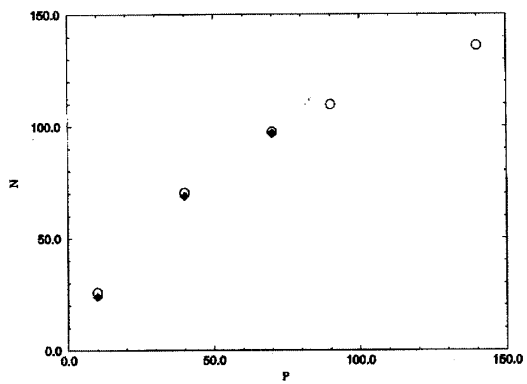

FIG. 3. Average numbers N_s and N_{exp} of H_2 molecules per unit cell of the zeolite computed by GCMC simulation (dot) (cf. Sec. III B) and measured experimentally (diamond) at $T=293$ K ($k_BT/\epsilon^{H_2H_2}=T^*=7.988$) with pressures ranging from 10 to 140 MPa.

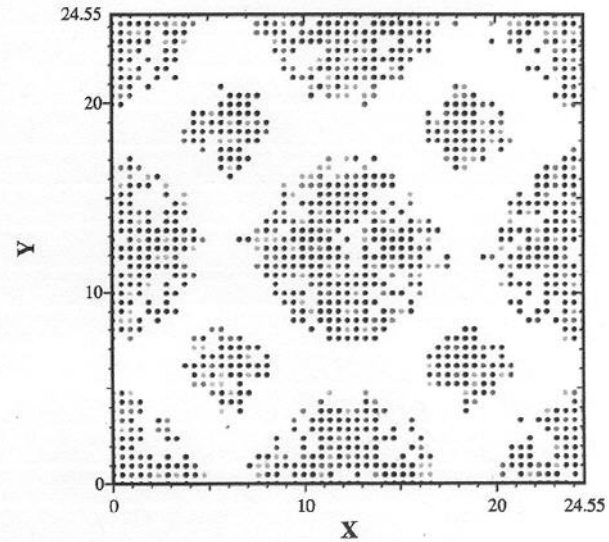

FIG. 4. Two-dimensional projection of the average local density of H_2 molecules in a unit cell of the NaA zeolite computed (cf. Sec. III B), at 10 MPa and $T^*=7.988$, from a GCMC simulation made of 2×10^6 MC steps. The dots show the domains where the average local density is different from zero. The shading of each dot indicates the value of the local density in a small subvolume of ~10 Å^3 around the dot position. The gray colors of the dots from white to black (black color is associated with the maximal local density) correspond to increasing values of the local density.

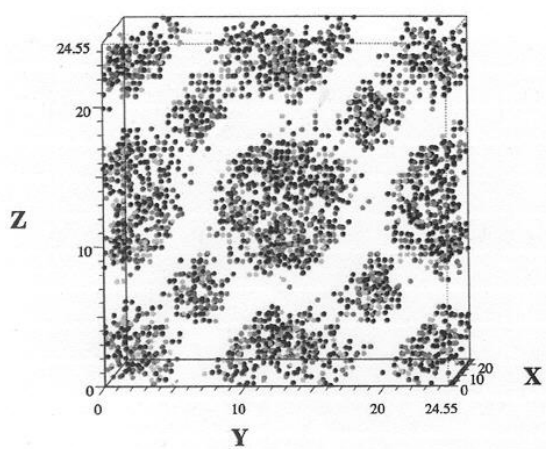

FIG. 5. Three-dimensional view of the average local density plotted in Fig. 4.

Modeling suggests that Zeolite A can store at least 2 wt.% H_2 if all cage sites are filled

F. Darkrim, A. Aoufi, P. Malbrunot, and D. Levesque, "Hydrogen Adsorption in the NaA Zeolite: A Comparison Between Numerical Simulations and Experiments", Journal of Chemical Physics, 112, 5991-5999 (2000).

Large Pore Zeolite UTD-1

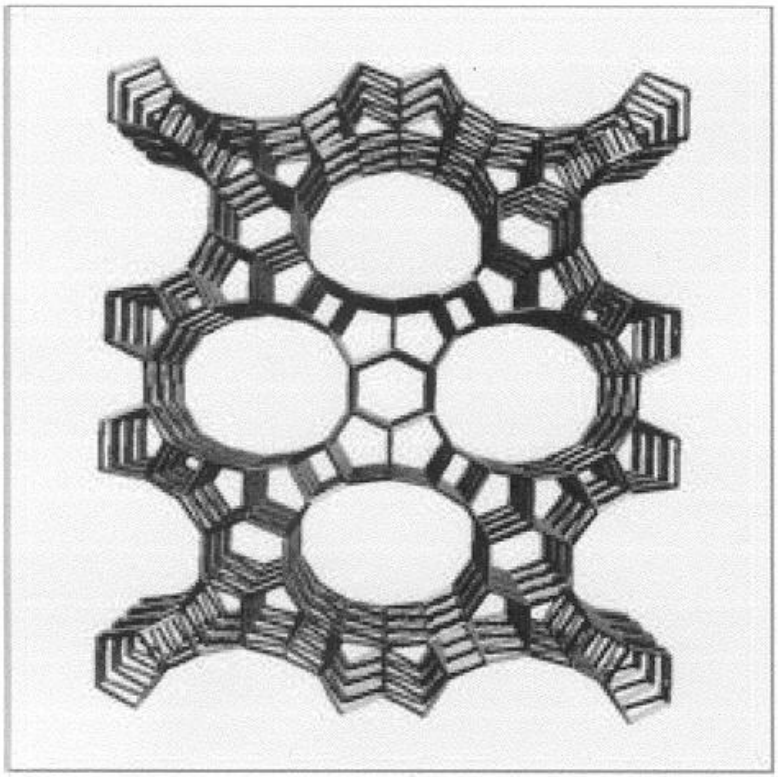

Figure 1. Framework structure of UTD-1 (oxygen atoms omitted for clarity) calculated with use of the crystallographic data in ref 38.

- **High silica zeolite**
  - **SiO_2/Al_2O_3 ratio ~ 70**
- **14-ring channel**
- **One-dimensional channel along [001]**
- **Channel dimensions of 1.0 x 0.75 nm**

Hydrogen storage in large pore zeolites has never been examined

R.F. Lobo, et.al., "Characterization of the Extra-Large-Pore Zeolite UTD-1", J. Am. Chem. Soc., 119, 8474-8484 (1997).

Mesoporous MCM-41 Material

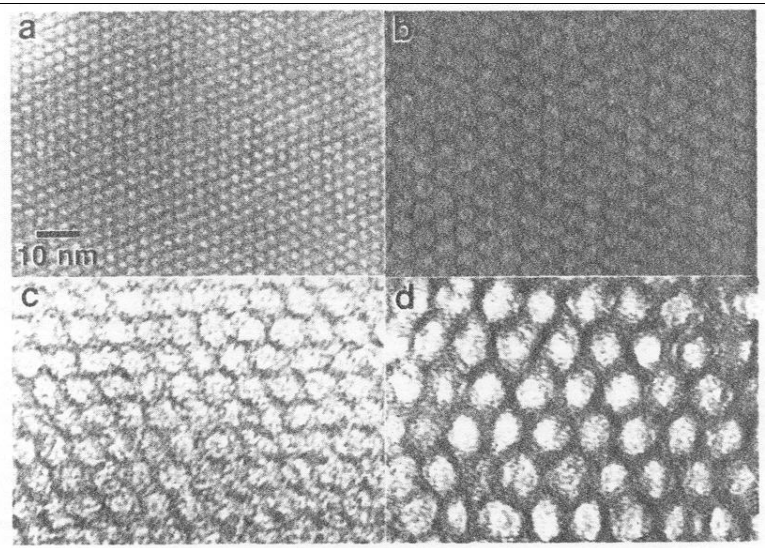

Figure 2. Transmission electron micrographs of several MCM-41 materials having Ar pore sizes of (a) 20, (b) 40, (c) 65, and (d) 100 Å.

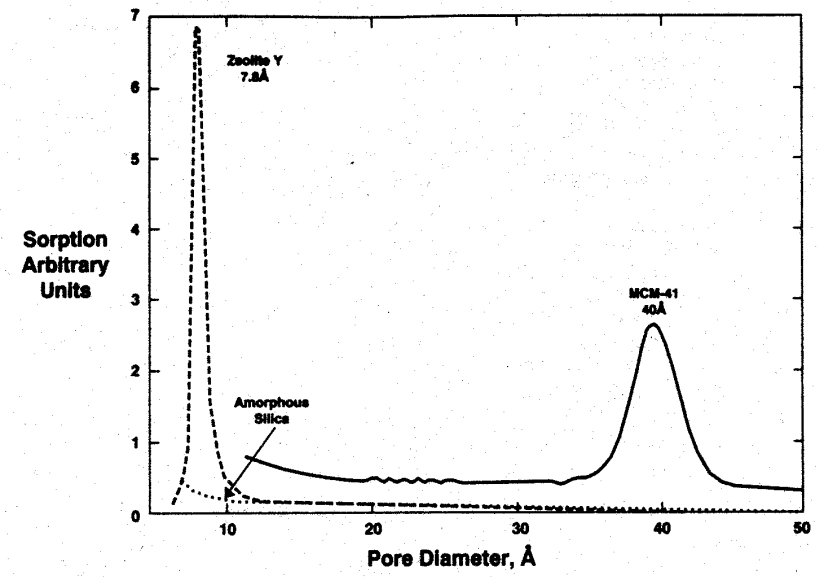

Horváth-Kawazoe pore size distributions for MCM-41(40), zeolite Y, and amorphous silica.

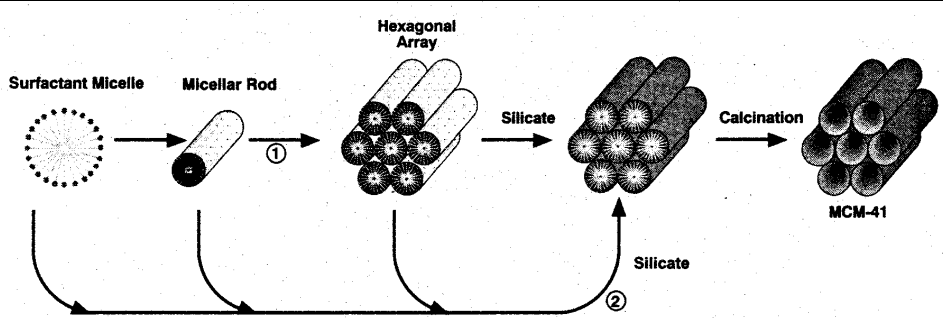

Figure 14. Possible mechanistic pathways for the formation of MCM-41: (1) liquid crystal phase initiated and (2) silicate anion initiated.

- Hexagonal array of uniform mesoporous channels ranging from 2-10 nm

J.S. Beck, et.al., "A New Family of Mesoporous Molecular Sieves Prepared With Liquid Crystal Templates", J. Am. Chem. Soc., 114, 10834-10843 (1992).

Synthesis of Ordered Carbon Molecular Sieves by Templating

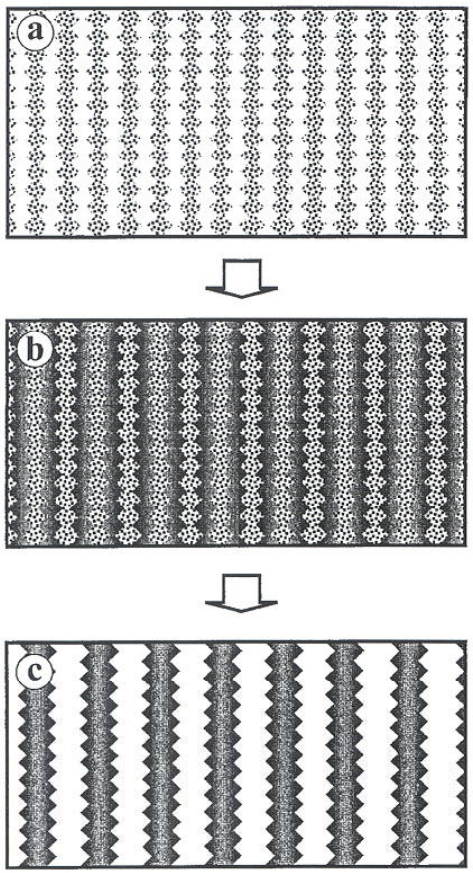

Figure 3. Schematic outline of the template synthesis procedure with silica molecular sieve: (a) The mesoporous silica molecular sieve MCM-48, (b) MCM-48 after completing carbonization within pores, and (c) CMK-1 obtained by removing the silica wall after carbonization.

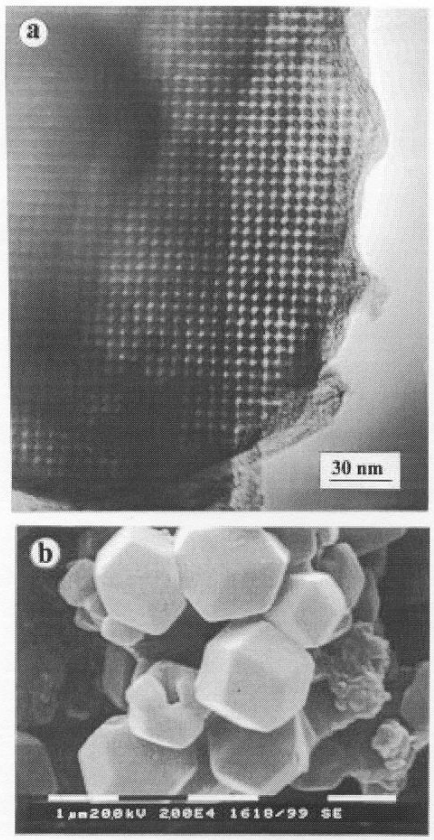

Figure 1. (a) Representative transmission electron micrograph of the ordered carbon molecular sieve CMK-1, obtained by the template synthesis with the mesoporous silica molecular sieve MCM-48. This image was obtained with a Philips CM20 transmission electron microscope operated at 100 kV from thin edges of a particle supported on porous carbon grid. (b) Scanning electron micrograph of a CMK-1 sample. This image was obtained on a Philips SEM-535M microscope using an acceleration voltage of 20.0 kV.

- Mesoporous silica molecular sieve MCM-48 impregnated with sucrose
- Sucrose converted to carbon by heating to 800-1100 ^{o}C in vacuum or inert atmosphere
- Silica framework dissolved in aqueous solution of NaOH and ethanol

R. Ryoo, S.H. Joo, and S. Jun, "Synthesis of Highly Ordered Carbon Molecular Sieves via Template-Mediated Structural Transformation", J. Phys. Chem. B, 103, 7743-7746 (1999).

SiO_2 Xerogels and Aerogels

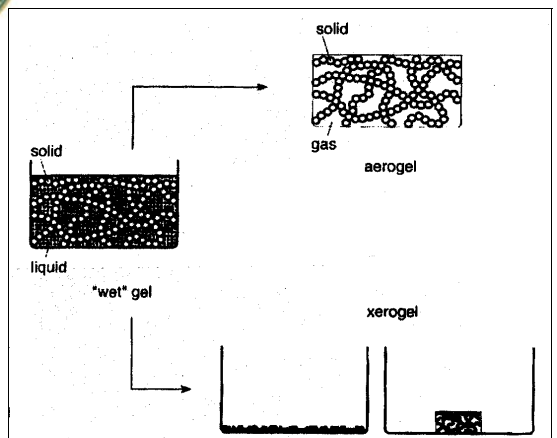

Figure 3. Shrinkage upon drying of a wet gel body to give an aerogel (top) and a xerogel (bottom) as a powder (left) and a monolith (right).

- **Xerogels**
  - Produced by conventional drying of wet silica gel
- **Aerogels**
  - Produced by liquid-to-gas drying of wet silica gel
    - Supercritical fluid drying

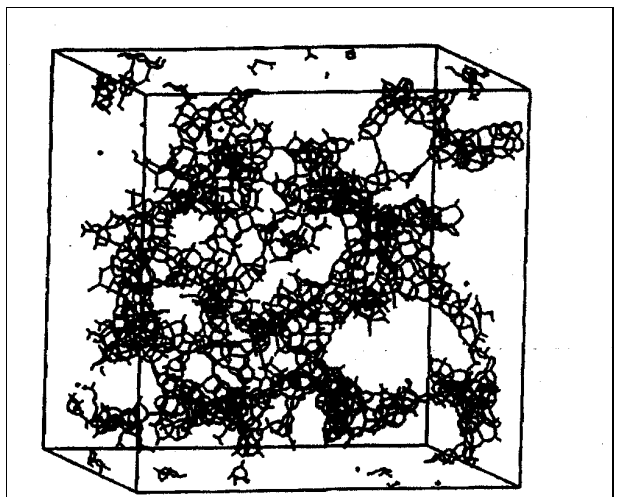

Figure 2. Schematic description of the structure of a silica aerogel (reproduced with friendly permission from ref. [6]).

Structural Properties of SiO_2 Aerogels

- Bulk density: 0.003-0.500 g/cm^3
- Porosity: 80% - 99.8%
- Mean pore diameter: 20-150 nm
- BET surface area: 100-1600 m^2/gm

N. Husing and U. Schubert, "Aerogels-Airy Materials: Chemistry, Structure, and Properties", Angew. Chem. Int. Ed., 37, 22-45 (1998).

Porous Metal-Organic MOF-5

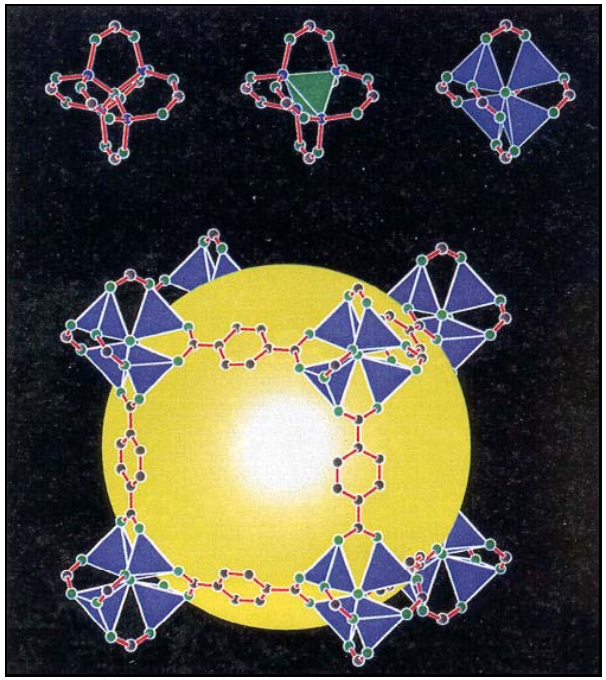

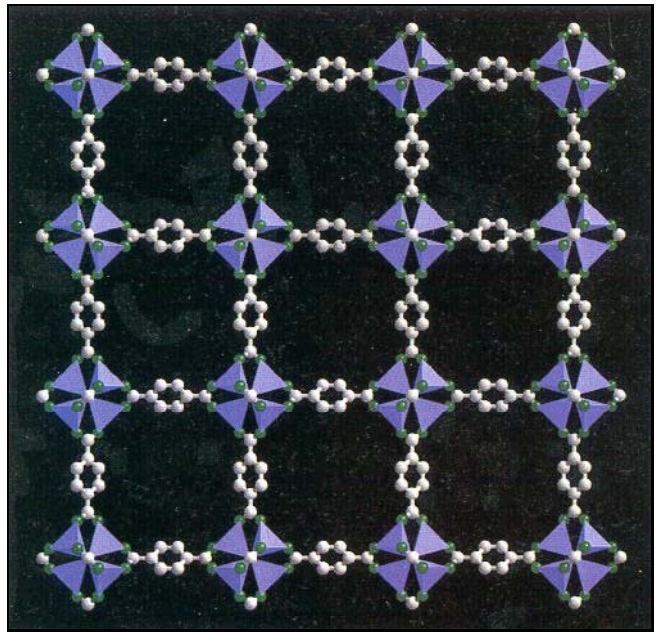

- Chemical formula $Zn_4O\ (BDC)_3\ (DMF)_8\ (C_6H_5Cl)$
  - BCD = 1,4 - benzenedicarboxylate
  - DMF = dimethylformamide
- ZnO_4 tetrahedral clusters linked together by C_6H_4-C-O_2 "struts"
- Cubic crystal structure
- 1.294 nm spacing between centers of adjacent clusters

H. Li, M. Eddaoudi, M. O'Keeffe, O.M. Yaghi, "Design and Synthesis of an Exceptionally Stable and Highly Porous Metal-Organic Framework", Nature, 402, 276-279 (1999).

Mesoporous Organosilica Material

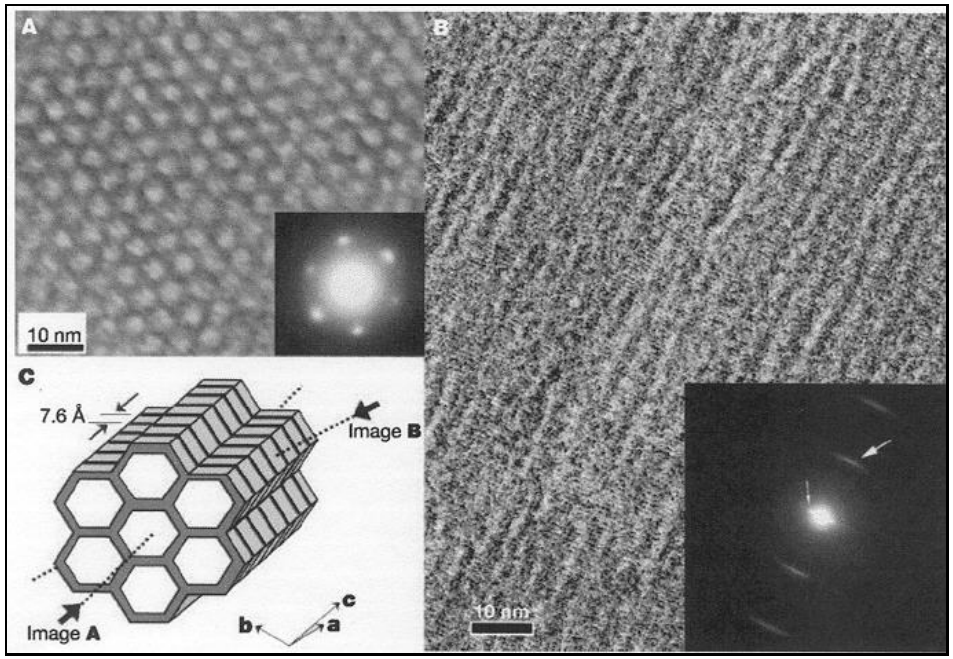

benzene-silica hybrid material

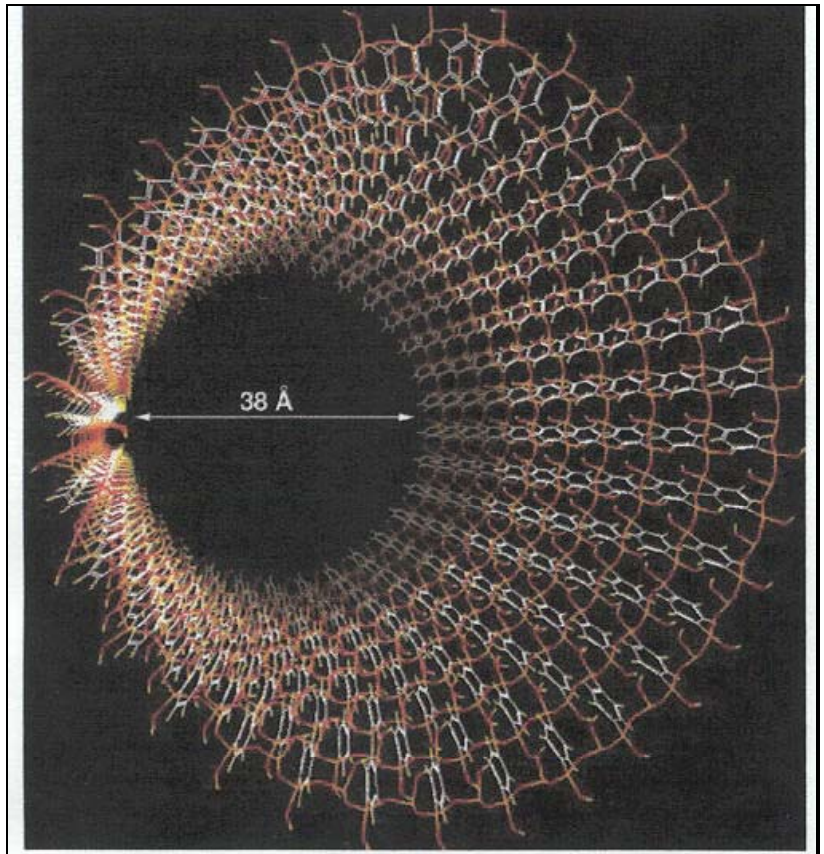

Figure 4 Model showing the pore surface of mesoporous benzene–silica. Benzene rings are aligned in a circle around the pore, fixed at both sides by silicate chains. The silicate is terminated by silanol (Si–OH) at the surface. Hydrophobic benzene layers and hydrophilic silicate layers array alternately at an interval of 7.6 Å along the channel direction. Silicon, orange; oxygen, red; carbon, white; hydrogen, yellow.

S. Inagaki, S. Guan, T. Ohsuna, and O. Terasaki, "An Ordered Mesoporous Organosilica Hybrid Material With a Crystal-Like Wall Structure", Nature, 416, 304-307 (2002).

Nanosize Metal and Ceramic Powders

- Nanosize metal and ceramic powders are commercially available
  - 10 - 100 nm diameters
- Nanosize metal powders
  - Au, Ag, Ni, Ti, Mo, Pt, W
- Nanosize ceramic powders
  - Al_2O_3, ZrO_2, CeO_2, CuO, MgO SiO_2, TiO_2

Gold-Thiol Single Molecule Electrical Junctions

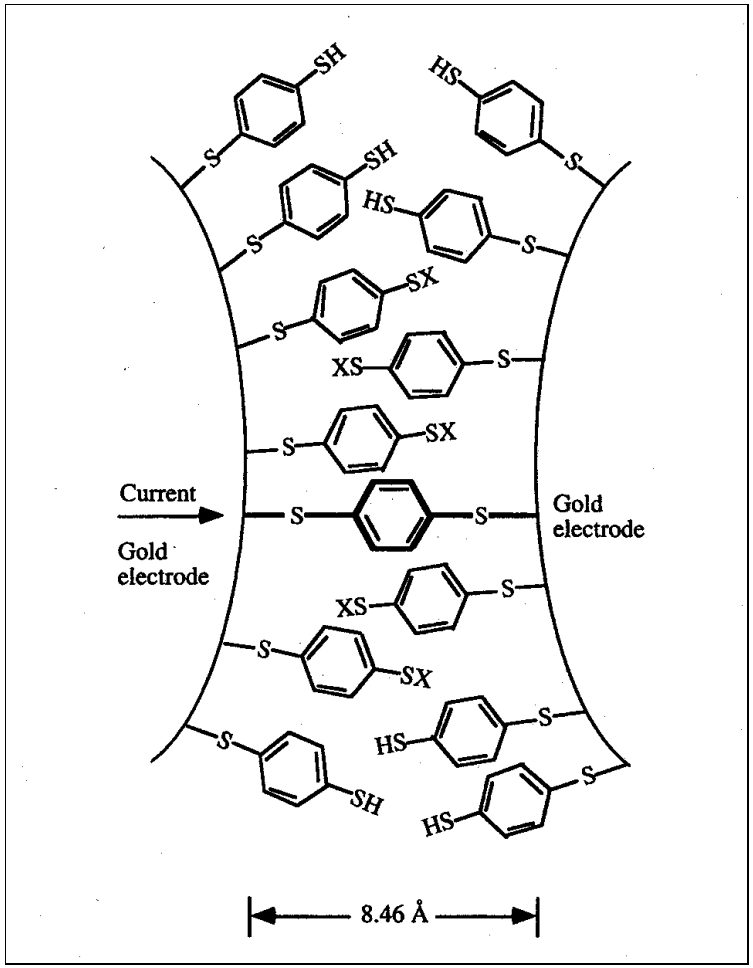

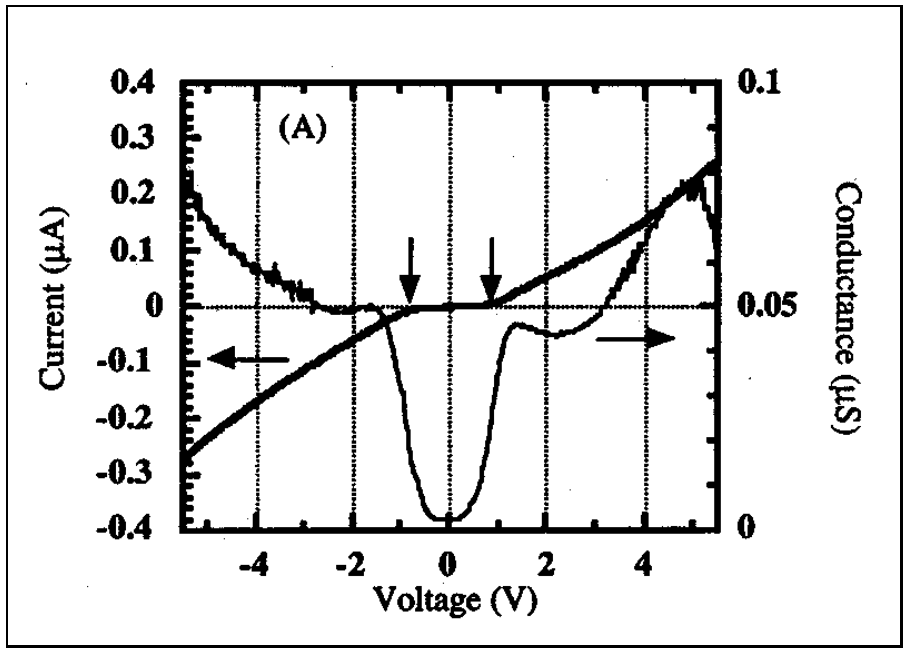

Single benzene-1,4-dithiolate molecule between atomically-sharp gold electrodes

M.A. Reed, C. Zhou, C.J. Muller, T.P. Burgin, and J.M. Tour, "Conductance of a Molecular Junction", Science, 278, 252-254 (1997).

Hydrogen Production by Grinding of Powders

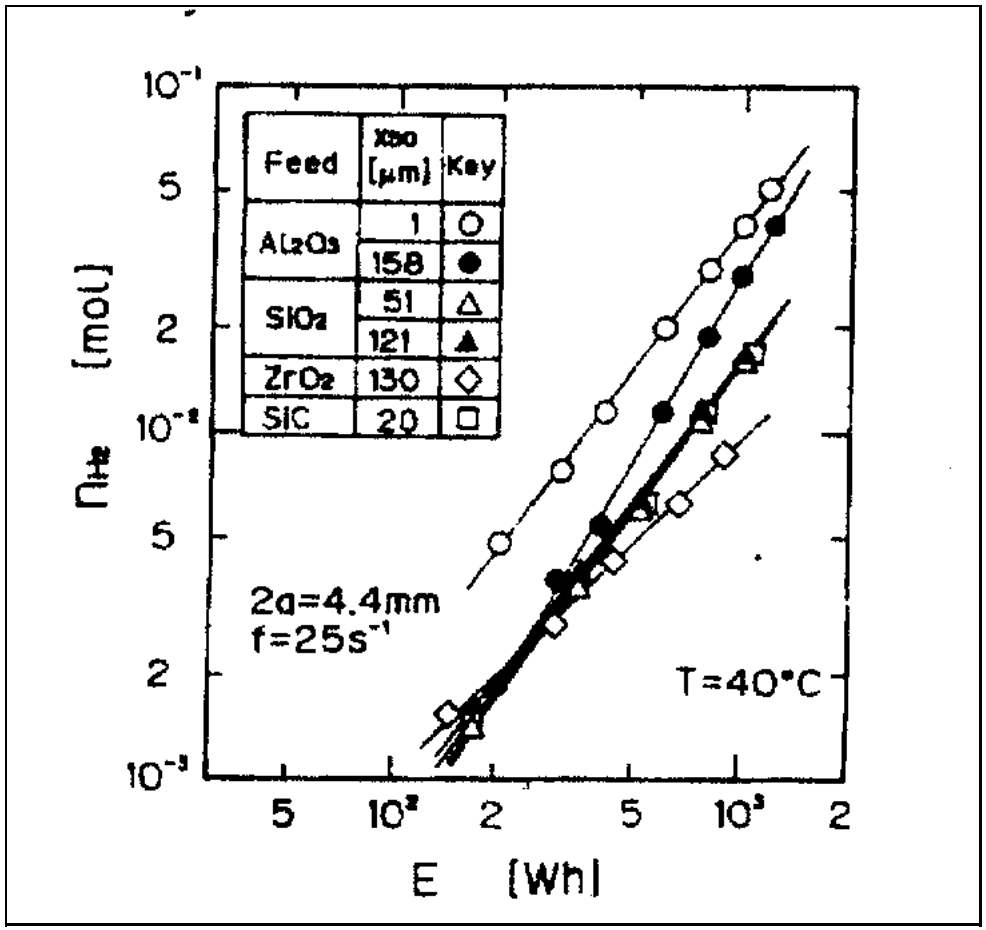

- "In wet grinding in liquid media including water or alcohol, it has been confirmed that a considerable amount of hydrogen is generated and causes an abnormal increase in pressure of a closed mill pot, even when the feed materials hardly react with them."
- Steel milling balls used to mill ceramic materials react with water to form hydrogen
- $\mathbf{3\ Fe + 4\ H_2O = Fe_3O_4 + 4\ H_2}$
  - 3.3 wt.% H_2 including both Fe and H_2O

T. Yokoyama, G. Jimbo, T. Nishimura, and S. Sakai, "Effect of Fineness of Wear Particles From Steel Balls on the Rate of Hydrogen Generation During Wet Grinding of Hard Materials in Water", Powder Technology, 73, 43-49 (1992).

Hydrogen Storage in Modified Iron Oxides

H_2 Storage: $Fe_3O_4 + 4H_2 = 3Fe + 4H_2O$

H_2 Recovery: $3Fe + 4H_2O = Fe_3O_4 + 4H_2$

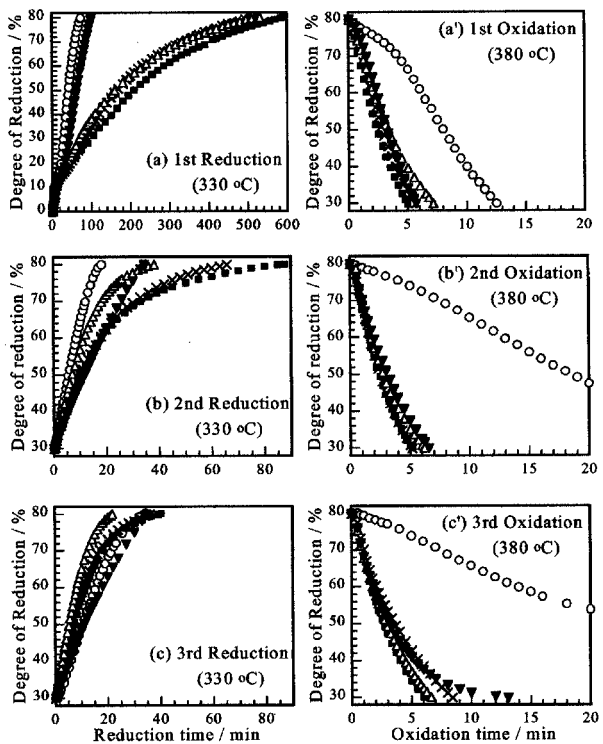

Fig. 1. Changes in the degree of reduction of Fe-oxides with and without additives as functions of reaction time for 1st to 3rd redox cycles. Additives: none (○), Ga (■), V (╳), Cr (△) and Mo (▼).

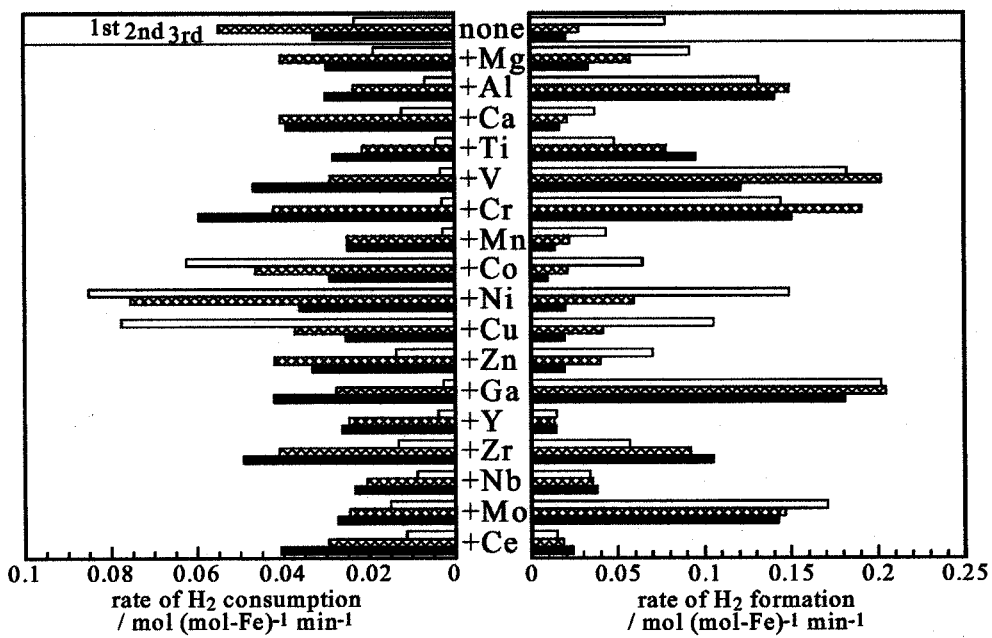

Fig. 2. Average rates of redox reactions for Fe-oxides with and without additives. Rate at 1st ( ), 2nd ( ) and 3rd ( ) cycles.

- **Additives accelerate reduction and oxidation reactions at lower temperatures**
  - **Al, Cr, Zr, Ga, V the most effective**

K. Otsuka, C. Yamada, T. Kaburagi, and S. Takenaka, "Storage and Generation of Pure Hydrogen by Utilization of Modified Iron Oxides", Proceedings, 14th World Hydrogen Energy Conference, June 2002, Montreal, Canada.

Effects of Mechanical Milling on Hydrogen Storage in Graphite

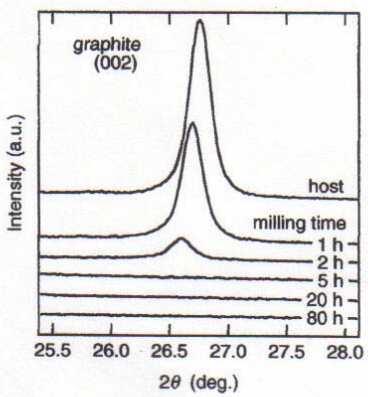

FIG. 1. (002) diffractions of the nanostructured graphite, that has been mechanically milled under initial hydrogen pressure of 1.0 MPa at room temperature.

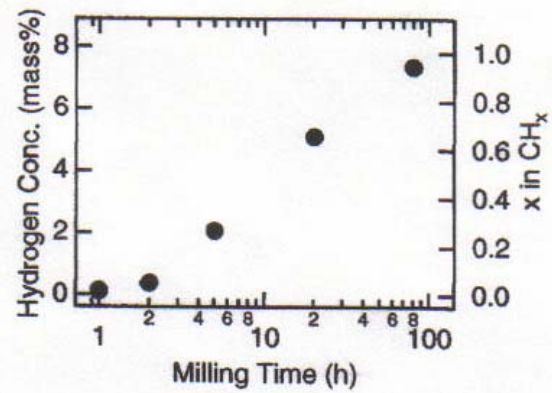

FIG. 2. Total hydrogen concentration in the nanostructured graphite, as a function of milling time under initial hydrogen pressure of 1.0 MPa at room temperature.

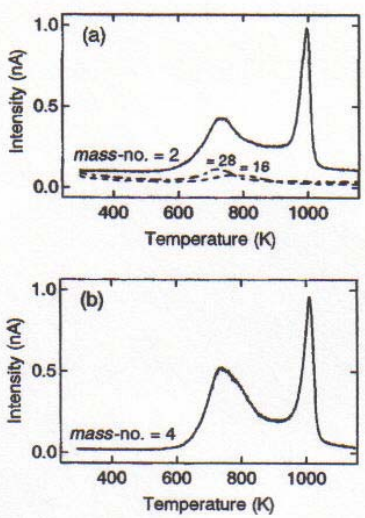

FIG. 3. TDS of nanostructured graphite mechanically milled under hydrogen (a) and deuterium (b) atmospheres, respectively.

- 200 μm graphite powder
- Planetary milling with steel balls and vial

S. Orimo, et.al., "Hydrogen in the Mechanically Prepared Nanostructured Graphite", Applied Physics Letters, 75, 3093-3095 (1999).

S. Orimo, et.al., "Hydrogen Desorption Property of Mechanically Prepared Nanostructured Graphite", Journal of Applied Physics, 90, 1545-1549 (2001).

Solubility of Hydrogen in Polymers

TABLE 18.2
Solubility of simple gases in polymers ($S(298)$ in cm^3 (STP)/$cm^3 \cdot$ bar = 10^{-5} cm^3(STP)/($cm^3 \cdot$ Pa)[1])

	N_2	O_2	CO_2	H_2	Heat of solution (ΔH_S in kJ/mol) N_2	O	CO_2	H_2
Elsatomers								
polybutadiene	0.045	0.097	1.00	0.033	4.2	1.3	−8.8	6.2
cis-1,4-polyisoprene (natural rubber)	0.055	0.112	0.90	0.037	2.1	−4.2	−12.5	–
polychloroprene	0.036	0.075	0.83	0.026	–	–	−9.6	6.2
styrene–butadiene rubber	0.048	0.094	0.92	0.031	0.3	2.3	–	–
butadiene–acrylonitrile rubber 80/20	0.038	0.078	1.13	0.030	5.8	2.0	−9.2	4.1
butadiene–acrylonitrile rubber 73/27	0.032	0.068	1.24	0.027	4.1	2.0	−10.8	4.1
butadiene–acrylonitrile rubber 68/32	0.031	0.065	1.30	0.023	4.6	0.8	−12.5	5.2
butadiene–acrylonitrile rubber 61/39	0.028	0.054	1.49	0.022	4	4.6	4.6	5.0
poly(dimethyl butadiene)	0.046	0.114	0.91	0.033	3.8	0.8	−6.6	2.0
polyisobutylene (butyl rubber)	0.055	0.122	0.68	0.036	1.7	−5.0	−8.8	2.5
polyurethane rubber	0.025	0.048	(1.50)	0.018	–	–	–	–
silicone rubber	0.081	0.126	0.43	0.047	–	–	–	–
Semicrystalline polymers								
polyethylene H.D.	0.025	0.047	0.35	–	2.1	−1.7	−5.3	–
polyethylene L.D.	0.025	0.065	0.46	–	7.9	2.5	0.4	–
trans-1,4-polyisoprene (Gutta-percha)	0.056	0.102	0.97	0.038	–	–	–	–
poly(tetrafluoroethylene)	–	–	0.19	–	−5.4	−7.2	−14.7	–
polyoxymethylene	0.025	0.054	0.42	–	–	–	–	–
poly(2,6-diphenyl-1,4-phenylene oxide)	0.043	0.1	1.34	–	–	–	–	–
poly(ethylene terephthalate)	0.039	0.069	1.3	–	−11.4	−13.0	−31.4	–
Glassy polymers								
polystyrene	–	0.055	0.65	–	–	–	–	–
poly(vinyl chloride)	0.024	0.029	0.48	0.026	7.1	1.3	−7.9	0
poly(vinyl acetate)	0.02	0.04	–	0.023	–	−4.6	−24.5	10.3
poly(bisphenol A-carbonate)	0.028	0.095	1.78	0.022	–	−12.9	−21.7	–

[1] Van Amerongen (1950, 1964) and Polymer Handbook.

Hydrogen has a very low solubility in polymers: ~ 0.0003 wt.% H_2 at 25 °C

D.W. Van Krevelen, "Properties of Polymers", Elsevier Scientific Publishing Company, New York, c. 1990.

Hydrogen Storage In Conducting Polymers

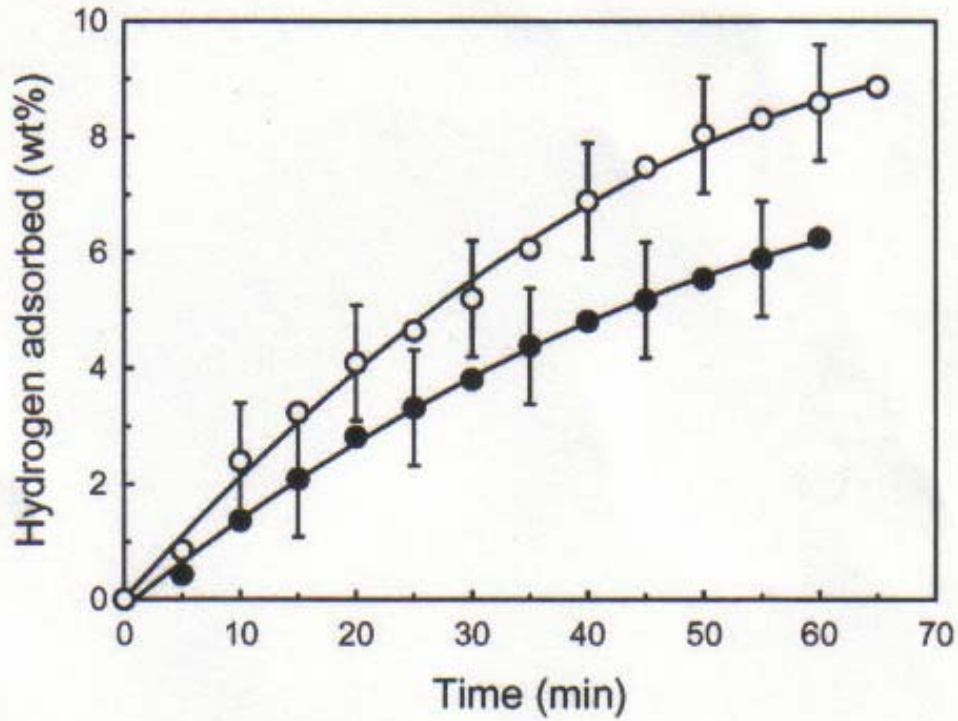

Figure 1. The amount of H_2 in wt % for both (●) the PANI and (○) the Ppy treated with concentrated hydrochloric acid. The measurement was started after evacuation at 473 K and subsequently at room temperature till at least 0.13 Pa.

S.J. Cho, K.S. Song, J.W. Kim, T.H. Kim, and K. Choo, "Hydrogen Sorption in HCl-TreatedPolyaniline and Polypyrrole: New Potential Hydrogen Storage Media", Fuel Chemistry Division Preprints, 47(1), xxxx (2002).

Next Steps

- Prepare workshop proceedings
- Hold workshop to address remaining R&D issues for compressed hydrogen tanks
- Update targets and draft 5-yr R&D Plan
- Draft hydrogen storage solicitation
- Accelerate development of standard test facility
- Discuss advanced storage concepts further to refine recommendations and resolve controversial aspects

For More Information

www.anl.gov/g8

www.cartech.doe.gov/publications/2002hydrogen

www.eren.doe.gov/hydrogen/news

www.hydpark.ca.sandia.gov